

# **Mitochondria are Dynamically Transferring between Human Neural Cells and Alexander Disease-associated GFAP Mutations Impair the Astrocytic Transfer**

**Longfei Gao<sup>1</sup>, Zhen Zhang<sup>1</sup>, Jing Lu<sup>1</sup>, and Gang Pei<sup>1, 2, 3, \*</sup>**

<sup>1</sup>State Key Laboratory of Cell Biology, CAS Center for Excellence in Molecular Cell Science, Shanghai Institute of Biochemistry and Cell Biology, Chinese Academy of Sciences; University of Chinese Academy of Sciences, Shanghai, China

<sup>2</sup>Shanghai Key Laboratory of Signaling and Disease Research, Collaborative Innovation Center for Brain Science, School of Life Sciences and Technology, Tongji University, Shanghai, China

<sup>3</sup>Institute for Stem Cell and Regeneration, Chinese Academy of Sciences, Beijing, China

\*Correspondence:

Dr. Gang Pei

[gpei@sibs.ac.cn](mailto:gpei@sibs.ac.cn)

## **Supplementary Information**

### Supplementary Figures

Supplementary Figure 1 Intercellular mitochondrial transfer between astrocytes.

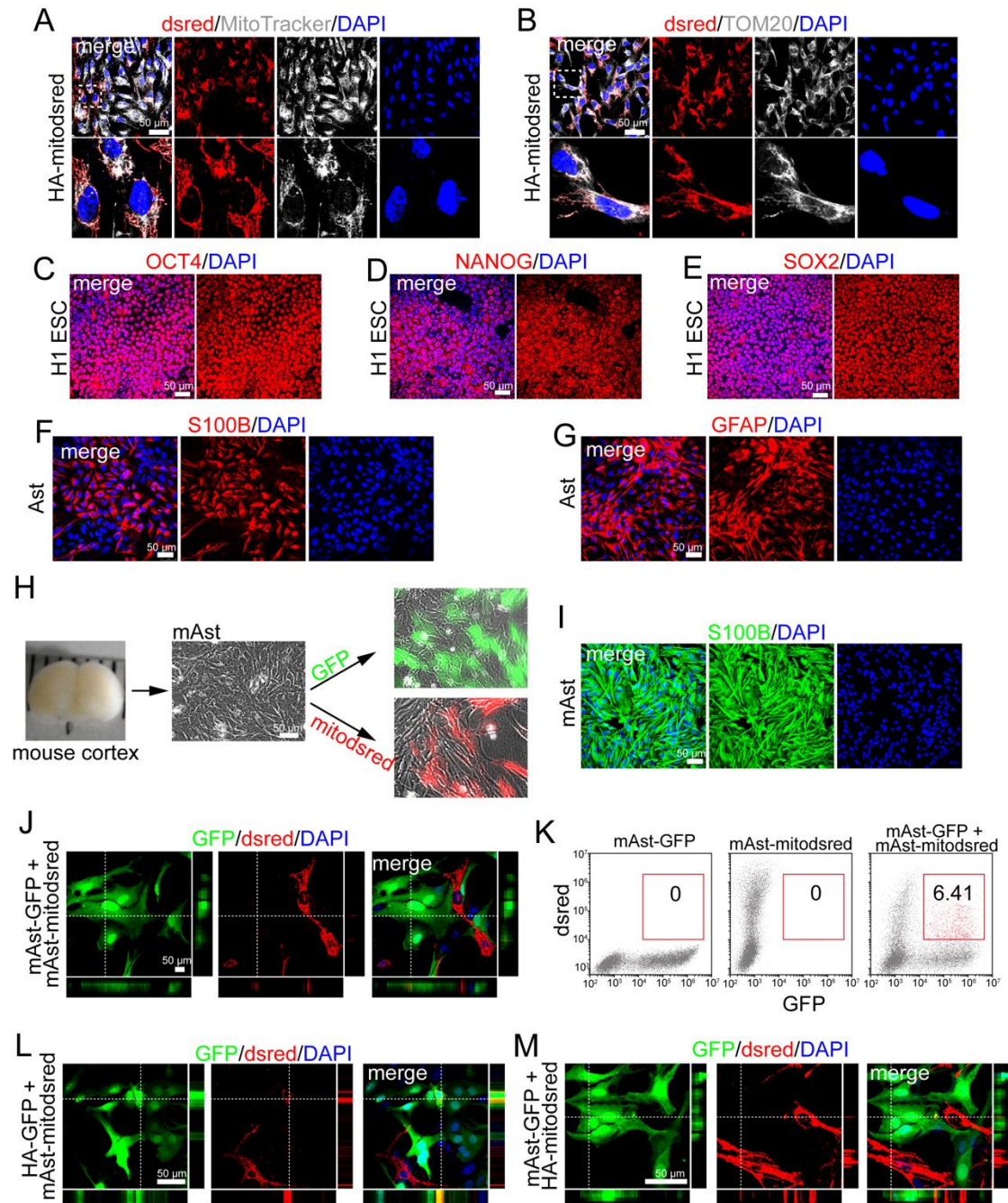
Supplementary Figure 2 Mitochondrial transfer from neuronal cells into astrocytes.

Supplementary Figure 3 Contribution of CD38/cADPR signaling and mitochondrial Rho GTPases to the transfer.

Supplementary Figure 4 Effects of mitochondrial transfer on recipient cells.

Supplementary Figure 5 Impaired mitochondrial transfer from astrocytes with GFAP mutations.

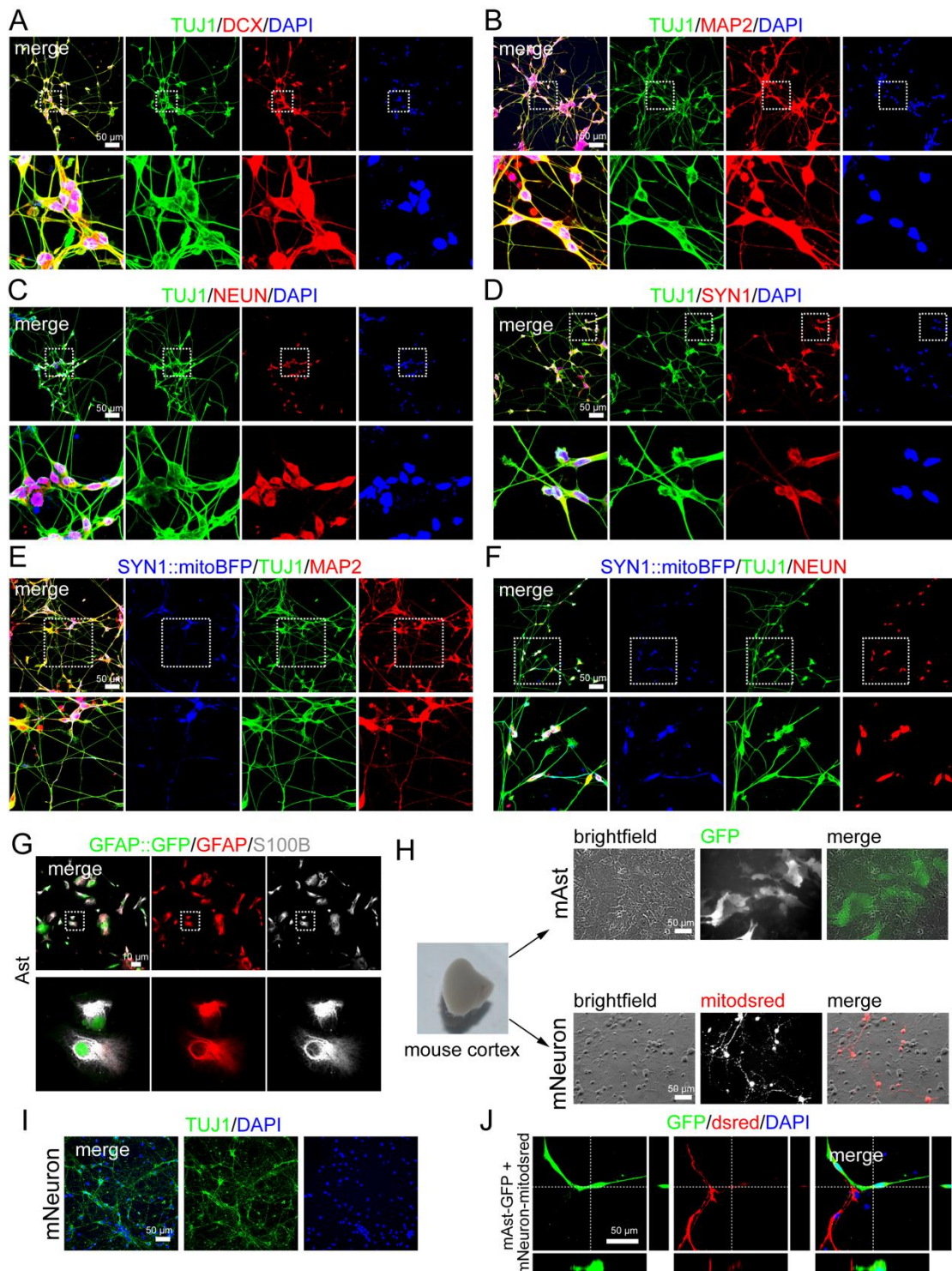
Supplementary Figure 6 Uncropped Western Blot images.



**Supplementary Figure 1 Intercellular mitochondrial transfer between astrocytes.**

(A-B) HA-mitodsred were stained with MitoTracker (Deep Red FM) (A) or anti-TOM20 antibody (B). (C-E) Immunostaining of OCT4 (C), NANOG (D), and SOX2 (E) on H1 ESCs. (F-G) Immunostaining of S100B (F) and GFAP (G) on H1 ESC-derived astrocytes. (H) Schematic images showing that primary mouse astrocytes (mAst) were derived from mouse cortex and labeled with GFP or mitodsred lentivirus. (I) Immunostaining of S100B on isolated mouse astrocytes. (J) mAst-GFP and mAst-mitodsred were co-cultured and mitochondria from mAst-mitodsred were observed in mAst-GFP after co-culture for 24 hours. (K) Flow cytometry analyzing mitochondrial transfer efficiency between mAst after co-cultured for 24 hours. (L) Mitochondria from mAst-mitodsred were observed in HA-GFP after co-cultured for 24 hours. (M)

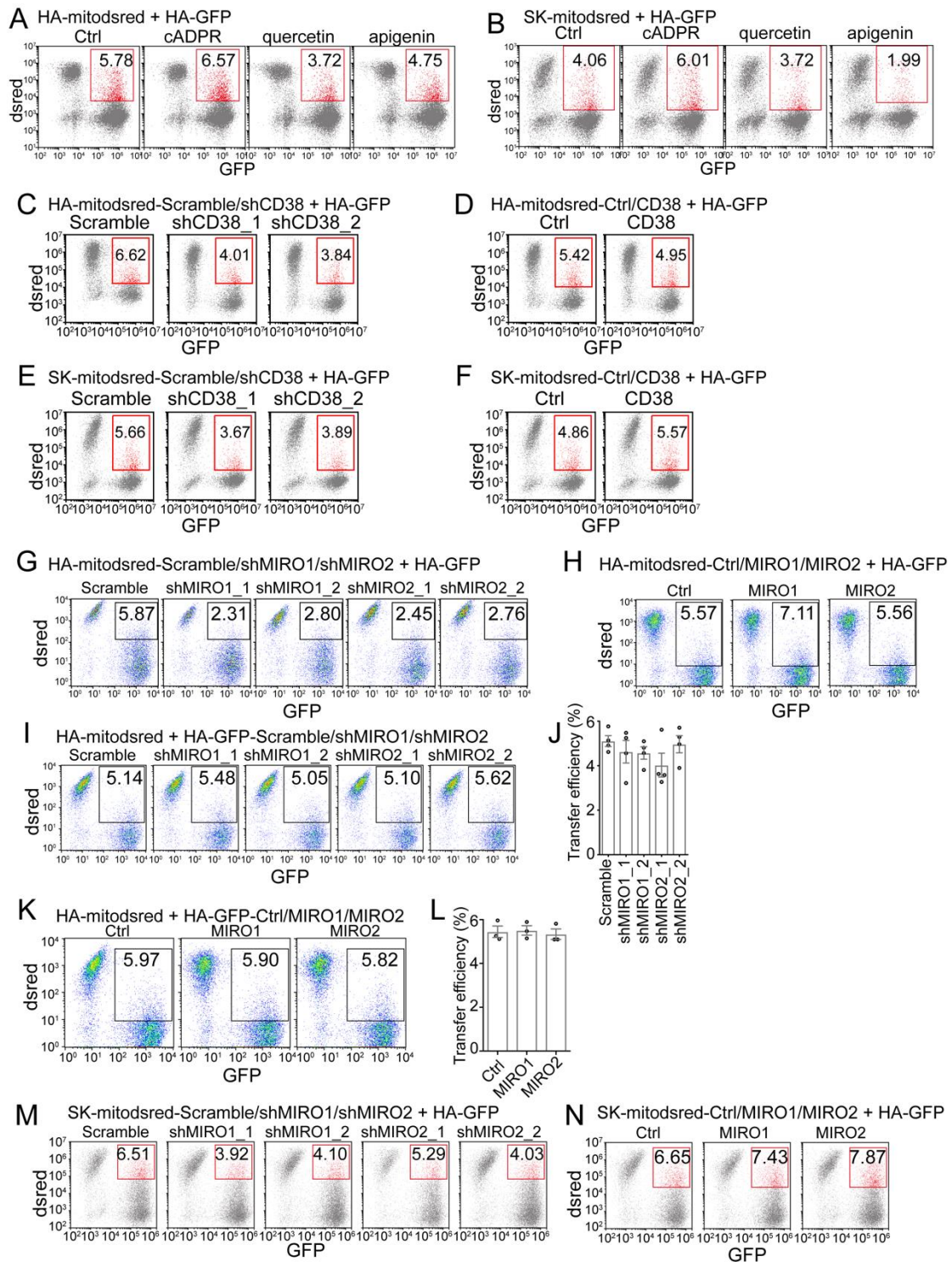
Mitochondria from HA-mitochondria were observed in mAst-GFP after co-cultured for 24 hours.



**Supplementary Figure 2 Mitochondrial transfer from neuronal cells into astrocytes.** (A-D) Immunostaining of TUJ1 (A, B, C, D), DCX (A), MAP2 (B), NEUN (C), and SYN1 (D) on hN. (E-F) Immunostaining of TUJ1 (E, F), MAP2 (E), and NEUN (F) on SYN1::mitoBFP labeled hN. (G) Immunostaining of S100B and GFAP on GFAP::GFP labeled Ast. (H) Primary mouse astrocytes (mAst) or neurons (mNeuron) were derived from mouse cortex. Lentivirus expressing GFP or mitodsred was used to label mAst or mitochondria in mNeuron. (I) Immunostaining of TUJ1 on mNeuron. Above 90% cells were positive for TUJ1. (J) Confocal images showing that

mitochondria from mNeuron-mitodsred were observed in mAst-GFP after co-cultured for 48 hours.

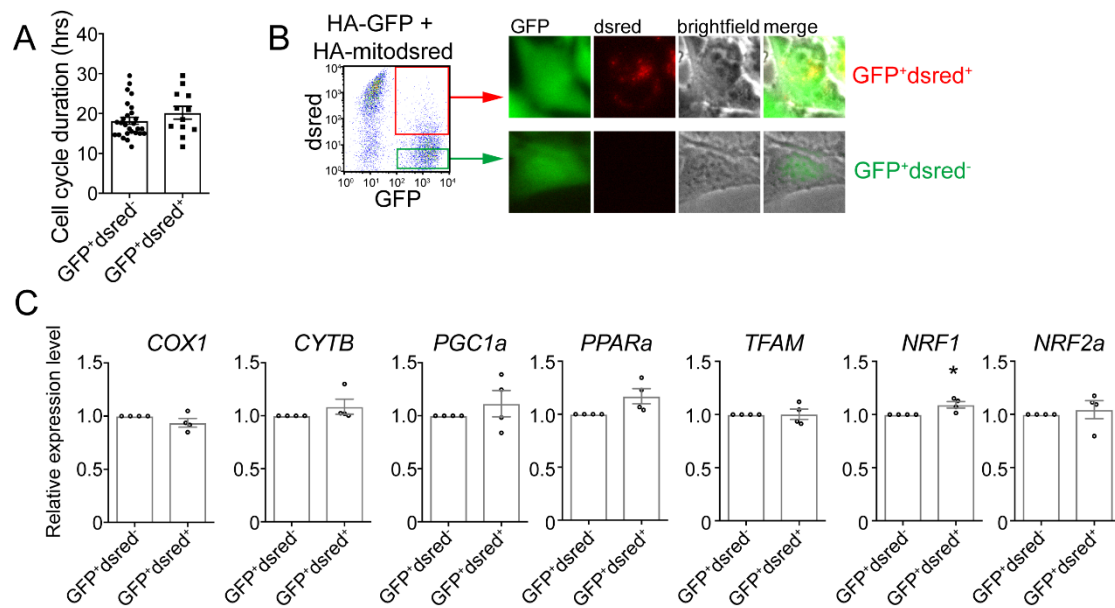




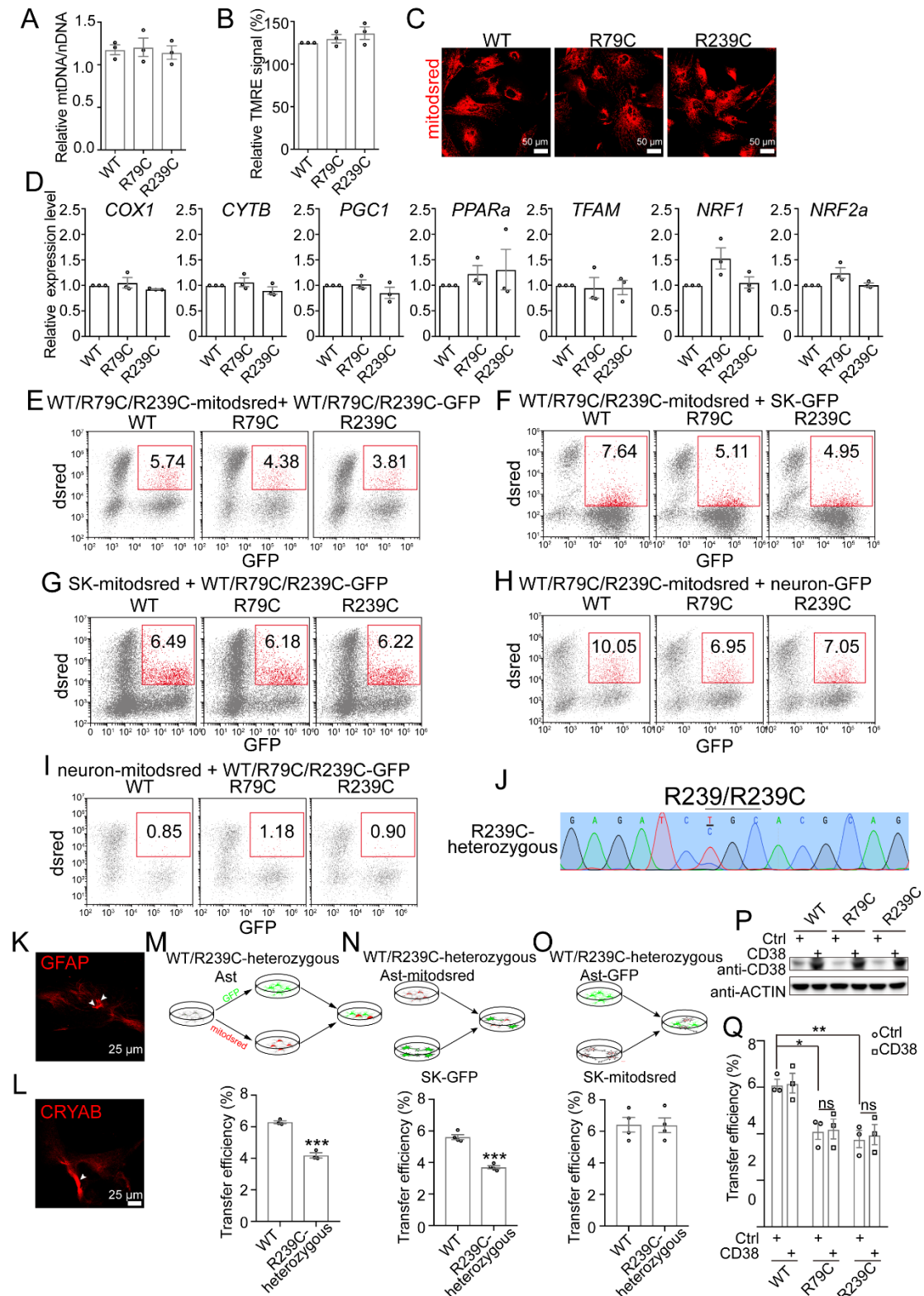
**Supplementary Figure 3 Contribution of CD38/cADPR signaling and mitochondrial Rho GTPases to the transfer.** (A) Representative flow cytometry results showing mitochondrial transfer between HA with indicated chemical treatment. (B) Representative flow cytometry results showing mitochondrial transfer from SK-mitodsred into HA-GFP with indicated chemical treatment. (C) Representative flow cytometry results showing mitochondrial transfer from HA-mitodsred transduced with scramble or CD38 shRNA into HA-GFP. (D) Representative flow cytometry results showing mitochondrial transfer from HA-mitodsred transduced with CD38 into HA-

GFP. **(E)** Representative flow cytometry results showing mitochondrial transfer from SK-mitodsred transduced with scramble or CD38 shRNA into HA-GFP. **(F)** Representative flow cytometry results showing mitochondrial transfer from SK-mitodsred transduced with CD38 into HA-GFP. **(G)** Representative flow cytometry results showing mitochondrial transfer from HA-mitodsred transduced with scramble, MIRO1, or MIRO2 shRNA into HA-GFP. **(H)** Representative flow cytometry results showing mitochondrial transfer from HA-mitodsred transduced with MIRO1 or MIRO2 into HA-GFP. **(I-J)** Flow cytometry analyzing mitochondrial transfer from HA-mitodsred into HA-GFP transduced with indicated shRNA. (Adjusted *p* values in J: Scramble vs. shMIRO1\_1, 0.8182; Scramble vs. shMIRO1\_2, 0.7604; Scramble vs. shMIRO2\_1, 0.2264; Scramble vs. shMIRO2\_2, 0.9971.) **(K-L)** Flow cytometry analyzing mitochondrial transfer from HA-mitodsred into HA-GFP transduced with indicated genes. (Adjusted *p* values in L: Ctrl vs. MIRO1, 0.9776; ctrl vs. MIRO2, 0.9277.) **(M)** Representative flow cytometry results showing mitochondrial transfer from SK-mitodsred transduced with indicated shRNA into HA-GFP. **(N)** Representative flow cytometry results showing mitochondrial transfer from SK-mitodsred transduced with indicated genes into HA-GFP. Data are represented as mean  $\pm$  SEM. Data are represented as mean  $\pm$  SEM. One-way ANOVA followed Dunnett's multiple comparisons test was applied in J and L.





**Supplementary Figure 4 Effects of mitochondrial transfer on recipient cells. (A)** Comparison of cell cycle duration between HA without transferred mitochondria (GFP<sup>+</sup>dsred<sup>-</sup>) and HA with transferred mitochondria (GFP<sup>+</sup>dsred<sup>+</sup>). No statistics difference was observed. ( $p = 0.2427$ . Two-tailed student t test.) **(B)** Separation of GFP<sup>+</sup>dsred<sup>-</sup> and GFP<sup>+</sup>dsred<sup>+</sup> cells by FACS. **(C)** Comparison of expression levels of mitochondrial biogenesis and metabolism markers between GFP<sup>+</sup>dsred<sup>-</sup> and GFP<sup>+</sup>dsred<sup>+</sup> cells. ( $p$  values, *COX1*, 0.1813; *CYTB*, 0.2709; *PGC1a*, 0.3932; *PPARa*, 0.0552; *TFAM*, 0.9474; *NRF1*, 0.0238; *NRF2a*, 0.617. Two-tailed student t test.) Data are represented as mean  $\pm$  SEM.



**Supplementary Figure 5 Impaired mitochondrial transfer from astrocytes with GFAP mutations.** (A-B) Comparison of mitochondrial DNA copy number (A) and MMP (B) among WT, R79C, and R239C astrocytes. (Adjusted  $p$  values with one-way ANOVA followed Dunnett's multiple comparisons test: A, WT vs. R79C, 0.9576; WT vs. R239C, 0.9477. B, WT vs. R79C, 0.7413; WT vs. R239C, 0.2786.) (C) Representative images showing representative mitochondrial morphology in WT,

R79C, or R239C astrocytes. **(D)** Comparison of expression levels of mitochondrial biogenesis and metabolism markers among WT, R79C, and R239C astrocytes. (Adjusted  $p$  values  $>0.05$ , one-way ANOVA followed Dunnett's multiple comparisons test.) **(E)** Representative flow cytometry images showing mitochondrial transfer efficiency between WT, R79C, or R239C astrocytes. Cells co-cultured for 24 hours were analyzed. **(F)** Representative flow cytometry images showing intercellular mitochondrial transfer efficiency from WT, R79C, or R239C astrocytes into SK-GFP. Cells co-cultured for 24 hours were analyzed. **(G)** Representative flow cytometry images showing intercellular mitochondrial transfer efficiency from SK-mitodsred into WT, R79C, or R239C astrocytes. Cells co-cultured for 24 hours were analyzed. **(H)** Representative flow cytometry images showing intercellular mitochondrial transfer efficiency from WT, R79C, or R239C astrocytes into primary mouse neurons. Cells co-cultured for 24 hours were analyzed. **(I)** Representative flow cytometry images showing intercellular mitochondrial transfer efficiency from primary mouse neurons into WT, R79C, or R239C astrocytes. Cells co-cultured for 24 hours were analyzed. **(J)** Sanger sequencing validating R239C heterozygous mutation in GFAP gene in H1 ESCs. **(K-L)** Representative images showing GFAP aggregates **(K)** and CRYAB **(L)** (indicated by white arrowheads) in R239C heterozygous astrocytes. **(M)** Flow cytometry analyzing mitochondrial transfer efficiency between WT or R239C heterozygous astrocytes. Cells co-cultured for 24 hours were analyzed ( $p<0.001$ , unpaired two-tailed student t test). **(N)** Flow cytometry analyzing intercellular mitochondrial transfer efficiency from WT or R239C heterozygous astrocytes into SK-GFP. Cells co-cultured for 24 hours were analyzed ( $p<0.001$ , unpaired two-tailed student t test). **(O)** Flow cytometry analyzing intercellular mitochondrial transfer efficiency from SK-mitodsred into WT or R239C heterozygous astrocytes. Cells co-cultured for 24 hours were analyzed ( $p=0.9653$ , unpaired two-tailed student t test). **(P)** Western blotting showing overexpression of CD38 in WT, R79C, or R239C astrocytes. **(Q)** Flow cytometry analyzing mitochondrial transfer between WT, R79C, or R239C astrocytes with or without overexpression of CD38. Cells co-cultured for 24 hours were analyzed (Adjusted  $p$  values with two-way ANOVA followed Tukey's multiple comparisons test: WT-ctrl vs. R79C-ctrl, 0.0273; WT-ctrl vs. R239C-ctrl, 0.0094; WT-ctrl vs. WT-CD38, 0.999; R79C-ctrl vs. R79C-CD38,  $>0.999$ ; R239C-ctrl vs. R239C-CD38, 0.999.) Data are represented as mean  $\pm$  SEM. ns, no significance.

Figure 3

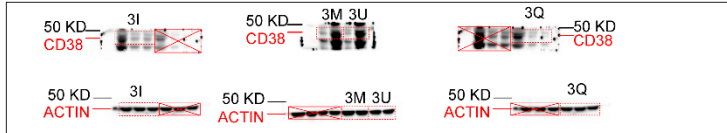


Figure 4C & 4G

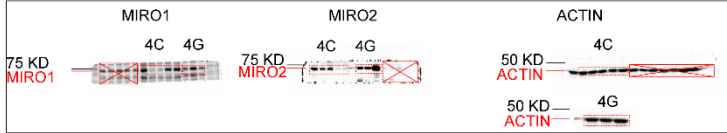


Figure 4K

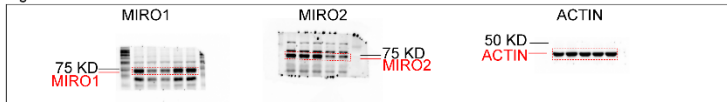


Figure 4O

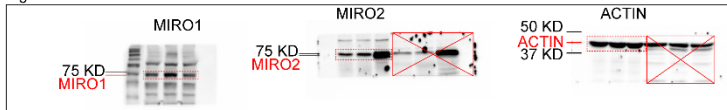


Figure 6M



**Supplementary Figure 6 Uncropped Western Blot images.**